

Transport through the network of topological channels in HgTe based quantum well

G. M. Gusev,¹ Z. D. Kvon,^{2,3} D. A. Kozlov,² E. B. Olshanetsky,² M. V. Entin,² and N. N. Mikhailov^{2,3}

¹*Instituto de Física da Universidade de São Paulo, 135960-170, São Paulo, SP, Brazil*

²*Institute of Semiconductor Physics, Novosibirsk 630090, Russia and*

³*Novosibirsk State University, Novosibirsk 630090, Russia*

(Dated: December 1, 2021)

Topological insulators represent a new quantum state of matter which is characterized by edge or surface states and an insulating band gap in the bulk. In a two dimensional (2D) system based on the HgTe quantum well (QW) of critical width random deviations of the well width from its average value result in local crossovers from zero gap 2D Dirac fermion system to either the 2D topological insulator or the ordinary insulator, forming a complicated in-plane network of helical channels along the zero-gap lines. We have studied experimentally the transport properties of the critical width HgTe quantum wells near the Dirac point, where the conductance is determined by a percolation along the zero-gap lines. The experimental results confirm the presence of percolating conducting channels of a finite width. Our work establishes the critical width HgTe QW as a promising platform for the study of the interplay between topology and localization.

INTRODUCTION

Topological states of matter have attracted a lot of attention due to their numerous intriguing transport properties. In particular, in two-dimensional topological insulators (2D TI) there are gapless conducting helical edge channels, that are protected against backscattering [1–5]. Many experiments have been performed to investigate the transport properties of the 2DTI edge states in several materials where the helical edge states are due to different physical mechanisms. For example the main factor responsible for the existence of a nontrivial topological phase in HgTe/CdTe quantum wells (QW) is a strong spin-orbit interaction [6–11], whereas in InAs/GaSb double QWs the topologically protected helical edge states in the inverted phase emerge as a consequence of the coupling between the bands leading to the opening of a hybridization gap [12–16]. As has been verified on many occasions (for review see [17]) generally two basic experimentally observed features indicate the presence of ballistic helical edge channels in submicron 2DTI samples: the conductance of the order of the universal value e^2/h [6, 10] and a strong nonlocal signal due to the helical edge states current circulating along the sample perimeter [8–11].

The interplay between topology and localization is another challenging object of study both for theoreticians and experimentalists. To gain a deeper insight into the critical behaviour of matter, theoreticians often employ network models. Such is the case for the metal-insulator transition and also for the transition between different phases of topological insulator [18–23]. Critical phenomena related to the integer and fractional quantum Hall effects have been successfully described by a chiral Chalker-Coddington-like network representation of bulk transport in the high magnetic field limit [24]. In contrast to the quantum Hall states, the two-dimensional topological insulator-metal transition could be represented by

uncoupled counter propagating channels with opposite spin, the so called Z_2 network model [18, 19, 21–23].

It was recognized that for topological metallic states a well-defined mobility edge, i.e. a specific energy separating the region of extended states from that of the localized states, is expected, while the extended states in quantum Hall effect are located at particular distinct energy values (no mobility edge).

As already mentioned, a network of conducting channels occurs naturally in HgTe quantum wells of critical width $w_c \approx 6.3nm$. It has been shown [6, 7] that if the HgTe QW width is below the critical value, the system is an ordinary insulator with a normal energy band structure. If, on the other hand, the QW width is above the critical, then it is a 2D topological insulator with an inverted energy spectrum. Finally, the QW width $w = w_c$ corresponds to the 2D Dirac fermion system with a gapless, single-cone spectrum (Figure 1). In-plane fluctuations of the QW width about its average value $w = w_c$, that cannot be completely avoided during the QW growth, lead to spacial gap variations (random gap sign changes), and therefore, to transitions between the mentioned topological phases. This results in a network of zero energy channels running along the boundaries separating the normal insulator and the 2D topological insulator phases (Figure 1). In addition to the gap fluctuations there will also be variations of the electrostatic potential due to random distribution of charged impurities. For the Fermi energy located near the Dirac point the system conductivity is attributed to the percolation along zero energy channels [26, 27].

In the present paper we study the transport properties of the zero gap HgTe quantum well (QW of critical width) both for $B = 0$ and in the presence of magnetic field. We find that the conductivity of the samples lies in the interval $(1.5 - 4)e^2/h$, as is expected for the topological network formed by finite width conducting channels. In order to estimate the width of the channels we per-

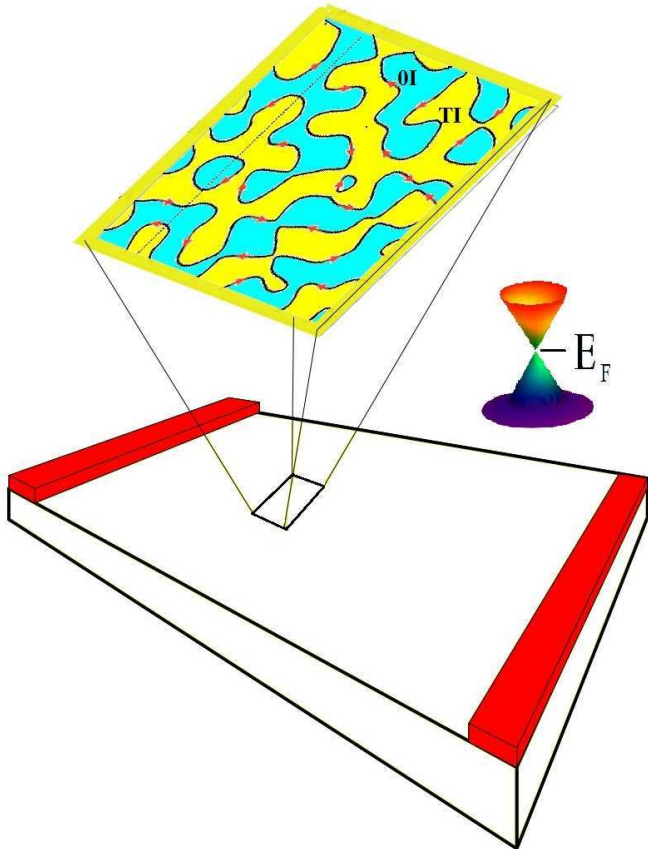


FIG. 1: (Color online) Schematic of zero energy topological channels in the slab shaped sample based on HgTe quantum well of a critical width $w_c \approx 6.3\text{nm}$. Yellow regions are topological insulator domains, blue regions correspond to ordinary insulator domains. The Dirac Fermions motion direction at a fixed spin projection is shown by arrows.

formed additional measurements of the Hall effect at low magnetic fields. Surprisingly, we find that the Hall effect near the percolation threshold is completely suppressed in a narrow interval of carrier densities in agreement with the percolation model [26, 27].

RESULTS AND DISCUSSION

Structural properties

Quantum wells $Cd_{0.65}Hg_{0.35}Te/HgTe/Cd_{0.65}Hg_{0.35}Te$ with (013) surface orientations and a nominal well thickness of (6.3-6.6) nm were prepared by molecular beam epitaxy (see Figures 2,3). Transmission electron microscopy (TEM) of cross sectional sample allows to study the interfaces of layered structures directly with a spatial resolution down to a nanometer scale. Figure 2a shows TEM images of the cross sections of the

specimen with designations of various layers constituting the structures, which allow assessment of abruptness of interfaces as well as lateral uniformity of layer growth [29]. The difference of contrasts in TEM images is due to the difference in the chemical compositions of the layers, which allows to determine the fluctuation of the width of the individual layers in the image of a multilayer structure. Both images indicate that HgTe/HgCdTe interfaces are reasonably abrupt. A histogram in Figure 2b is a display of statistical information on HgTe well width fluctuations. The histogram follows a normal Gaussian distribution with mean with $d_c \approx 6.1\text{nm}$ with standard deviation of 0.6 nm. As we mentioned above, the width fluctuations near topological transition lead to spacial gap variations, and therefore, to transitions between the topological phases.

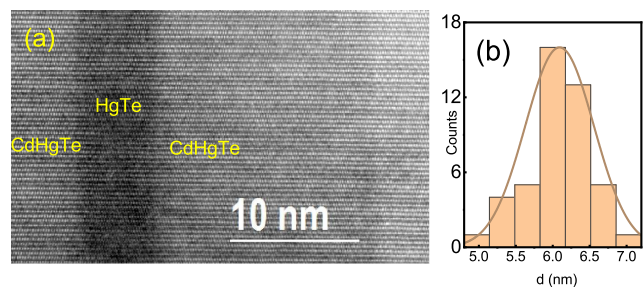


FIG. 2: (Color online) (a) TEM images of cross sections of sample. (b) Histogram displaying the distribution of well widths across the whole image.

sample	w (nm)	V_{CNP} (V)	$\rho_{max}(h/e^2)$	$\mu(V/cm^2s)$
1	6.3	-0.6	0.35	56.000
2	6.4	-1.28	0.27	90.000
3	6.3	-3	0.27	59.600
4	6.3	-4.3	0.31	58.600
5	6.3	-4.7	0.29	46.400

TABLE I: Some of the typical parameters of the electron system in HgTe quantum well at T=4.2K.

Gapless Dirac fermions and Drude conductivity

Recently it has been demonstrated that HgTe quantum well with a critical width $w_c = 6.3\text{nm}$ constitutes a system of 2D fermions with a single Dirac cone spectrum [28, 30–32]. The fluctuations of the QW width result in a random potential in the bulk of the QW. In QW of critical width these fluctuations lead to the formation of a random network of zero energy lines, as shown in Figure 1. We believe that the physical properties of this network are described by Z_2 quantum network model, and below we present experimental evidence that supports this assumption.

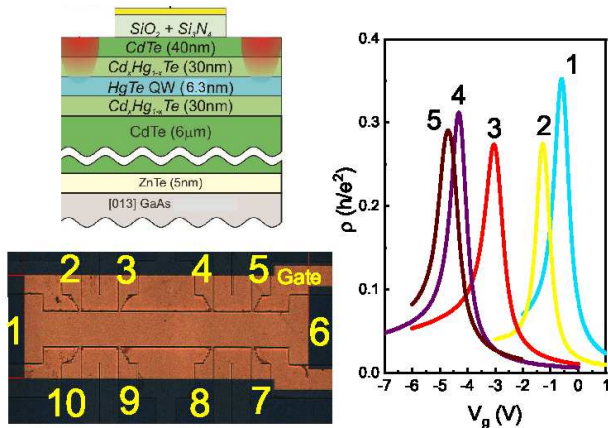


FIG. 3: (Color online) Resistance as a function of the gate voltage for different samples, $T=4.2K$. Left bottom- schematic structure of the sample. Right bottom - top view of the sample.

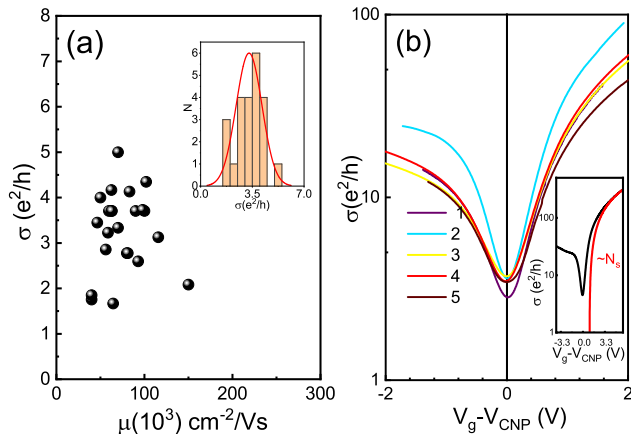


FIG. 4: (Color online)(a) The minimum conductivity and mobility at $n_s = 10^{11}cm^{-2}$ for 24 samples. Insert- Histogram displaying the distribution of the conductivity minimum. (b) Conductivity of the five representative samples near the CNP as a function of V_g . Insert- conductivity of sample 1 in a wider range of the gate voltages. Red line-linear n_s dependence.

Devices for transport measurements (see chapter method) are specially designed for multi-terminal measurements and consists of three narrow ($50\mu m$ wide) consecutive segments of different length (100, 250, 100 μm) and seven voltage probes (see Figure 3, left bottom panel). A dielectric layer was deposited (100 nm of SiO_2 and 100 nm of Si_3Ni_4) on the sample surface and then covered by a TiAu gate (see Figure 3, left top panel). In conventional transport measurements the current is applied between contacts 1-6 and the potential difference is measured between contacts 2-3, 3-4 and 4-5 of the sample. Figure 3 shows the resistivity $\rho(Vg)$ at zero magnetic field for five samples fabricated from different wafers and

at different time. The table 1 lists the typical parameters of the devices, such as the well width w , the gate voltage corresponding to the Dirac point position V_{CNP} , the resistivity value at the CNP ρ_{max} and the electron mobility $\mu = \sigma/n_s e$ for the density $n_s = 10^{11}cm^{-2}$. The Figure 4a shows the conductivity distribution for 24 samples, grown during a five years period. One can see that the conductivity values lie in the interval $(1.5 - 4)e^2/h$. Figure 4b shows the conductivity as a function of gate voltage V_g for five representative samples with parameters listed in table 1. The $\sigma(V_g)$ dependence is symmetric and nearly parabolic close to the CNP for low electron densities ($n_s < 2 \times 10^{10}cm^{-2}$) and approximately linear in electron density for higher density values. It is convenient to consider the total conductivity as a sum of the network conductivity σ_{nw} and the bulk conductivity σ_{2D} : $\sigma_{tot} = \sigma_{nw} + \sigma_{2D}$.

Let us start our analysis with the bulk contribution to the conductivity. The unscreened Coulomb disorder induced by randomly distributed charge impurities has been considered as the dominant mechanism of scattering in HgTe quantum well because of a very large HgTe dielectric constant and small Dirac fermions effective mass. Two distinct transport regimes can be indicated. For large carrier density the Boltzmann transport theory is valid [34]. On approaching the Dirac point (low carrier density), at a certain energy there will be an Anderson transition from the higher energy delocalized states to the localized states in narrow impurity bands located in small direct or inverted energy gaps (see Figure 1). It would be reasonable to suppose that transport via the delocalized states near the boundary with the localized bands can be described using the ordinary expression for mobility of carriers with a parabolic spectrum in the presence of impurity scattering. In this case the mobility is given by $\mu = A(n_s/n_i)$, where n_i is the impurity density, $A = (\epsilon_s/e^3)(16\pi\hbar^3/m_{DF}^2)$, m_{DF} is the effective mass at the Fermi level [33]. We get $\sigma_{2D} = e\mu n_s$ with quadratic dependence on electron density for $n_s < 2 \times 10^{10}cm^{-2}$, as shown in Figure 4b. At higher electron densities the electron energy spectrum becomes linear and one has to use the transport time expression calculated in [34], which leads to a conductivity $\sigma(n_s)$ nearly linear with the electron density. Such conductivity behaviour is shown in Figure 4b.

Comparison with the network model

Transport in HgTe quantum wells of a critical width w_0 is believed to be governed by the energy gap fluctuations leading to the formation of the topological channels network (Figure 1). One can assume that the QW width fluctuations δw can be described by the Gaussian distribution around the medium width value w , which follows from TEM images of the sample (Figure 2).

The percolation network can be characterized by a dimensionless parameter $\xi = \text{erf}((w - w_0)/\sqrt{2\delta w})$, where $\text{erf}(x)$ is the complementary error function. The unavoidable QW width fluctuations lead to a sample breaking-up into domains with positive (the ordinary insulator (OI)) and negative (the topological insulator (TI)) gap signs. If $|w - w_0| \gg \delta w$ and $w > w_0$ ($\xi \rightarrow 1$), then rare OI domains are embedded in TI domains. If, on the other hand, $w < w_0$, $\xi \rightarrow 1$, then rare TI domains are embedded in OI domains. For $w \rightarrow w_0$ ($\xi \rightarrow \xi_c = 0.5$) these domains are mixed in approximately equal proportion.

At the CNP the low-temperature the bulk conductivity of the OI or the TI domains should be close to zero. However, in the immediate vicinity of the lines separating the OI and TI domains (the zero gap line (ZGL)) the QW is a nearly gapless conductor. In fact, any such ZGL can be considered as a quantum wire. The sample conductance will be non-zero if such a line runs from one end of the sample to the other. On approaching the percolation threshold there forms a whole network of ZGLs covering the entire sample.

If the gap fluctuations are smooth, the wire associated with the ZGL will have many 1D subbands occupied. The important point is that two of these subbands will be the Weil states with a linear dispersion topologically protected from electron backscattering. The Weil states are similar to the edge states in Bernevig-Hughes-Zhang model of the 2D TI edge. In a small ballistic sample the edge state yields a dissipationless conductance equal to the conductance quantum.

In a large random system with a size exceeding the QW width fluctuation correlation length the ZGLs form a dense network. In this case the 2D conductivity is a combination of the ideal conductance of a Weil state and the conductance associated with tunnelling between different ZGLs lying close to each other.

The hopping between the ZGLs is realized via intermediate Dirac states, which lowers the hopping energy (as compared to the total gap) and raises the hopping probability amplitude. In any case one can use the characteristic hopping length between different ZGLs as some given quantity. Our consideration is based on geometric fractal properties of ZGLs.

We suppose that in our sample $|\xi - \xi_c| \ll 1$ so that a network of OI and TI domains is formed and the ZGLs cover the entire sample. It is worth noting, however, that in a realistic random network of channels a low temperature non-zero 2D conductivity may occur only if electrons can tunnel between the adjacent channels, for which a finite channel width is required [27]. One can estimate that :

$$\frac{|w - w_c|}{w_c} \sim \left(\frac{\hbar v}{\alpha \xi w_c} \right)^r \quad (1)$$

where $\alpha = \partial\Delta(w)/\partial w|_{w=w_c}$, Δ is the rms energy gap

fluctuation value, v is the electron velocity, r is parameter, which is close to 0.45 [27]. The conductivity of the network can be estimated from the equation [27]:

$$\sigma = \frac{e^2 D}{2\pi\hbar v a} \sim \frac{e^2}{h} \left(\frac{\Delta a}{\hbar v} \right)^p \quad (2)$$

where $D \simeq av(\Delta a/\hbar v)^p$ is the diffusion coefficient, p is a coefficient close to 0.15. We estimate the corresponding HgTe QW parameters from [27]: $\hbar v = 560\text{meV}$; $\alpha \approx -8.75\text{meV/nm}$, $\Delta \approx |\alpha|\sqrt{w^2 - \bar{w}^2} \approx 4\text{meV}$, $a = 30\text{ nm}$.

Combining all parameters we obtain $\sigma(n_w) = (e^2/h)(1 \pm 0.1)$, which is smaller than the average experimental value $\sigma_{exp} = (e^2/h)(2.5 \pm 1)$. This disagreement can be diminished if one takes into account the edge states nonzero width. This results in new percolation paths and, correspondingly, in higher σ_{nw} values and also in a much stronger σ_{nw} dispersion in agreement with the experiment.

The percolation model [27] predicts a non-zero conductivity in a narrow width interval near the critical value w_c due to the suppression of backscattering of electrons propagating along ZGLs and the growing hopping between adjacent ZGLs as $\bar{w} \rightarrow w_c$. It is expected, that the network conductivity vanishes outside of this percolation threshold. One can estimate the energy and the charge density interval where percolation conductivity occurs. However, in the experiment the total conductivity does not show a crossover from $\sim e^2/h$ values to zero beyond the percolation threshold, expected from the network model. Instead we observe a smooth conductivity growth with density near the CNP (Figure 3 and Figure 4b). As we already discussed above, the percolation conductivity is short-circuited by the conductivity of the bulk electrons.

The Hall effect in topological channel system

The percolation model also predicts other characteristic peculiarities in the transport coefficients behavior as well. One of the key effects proving the presence of a network structure in the system studied is the quenching of the Hall effect at low magnetic field.

The Figures 5a,b show the Hall resistivity as a function of gate voltage and magnetic field. Figure ??b shows a number of representative $\rho_{xy}(B)$ curves for $V_g = V_{CNP}$, $V_g < V_{CNP}$ and $V_g > V_{CNP}$. One can see a very narrow $\Delta V_g \simeq 0.05V$ region near the CNP, where $\rho_{xy} \approx 0$. Figures 5 a,b show that the Hall resistivity is flat and close to zero in the interval of magnetic field $-0.1T < B < 0.1T$. So, according to experiment there is a quenching of the Hall effect at the CNP in the energy interval corresponding to the density variation $\delta n_s \sim 5 \times 10^9\text{cm}^{-2}$.

From the theoretical point of view one can treat this situation as follows. A curved 1D ZGL state can be

mapped on the QW plane using the coordinate $\mathbf{r}(s)$, where s is the length along the edge and $\mathbf{s} = d\mathbf{r}(s)/ds$ is the tangent to the curve. If we take the magnetic field $\mathbf{B} = (0, 0, B)$ and the corresponding vector potential $\mathbf{A} = \mathbf{B} \times \mathbf{s}$ then the Hamiltonian of an electron in the 1D ZGL state will be $H = \sigma v_F (p - e[\mathbf{B} \times \mathbf{r}(s)]s/c)$, where σ is a spin index and v_F is the Fermi velocity. The gauge transform $U = \exp(i(e/c) \int [\mathbf{B} \times \mathbf{r}(s)] ds)$ converts the Hamiltonian H to σp . In this way, as one can see, the magnetic field can be effectively eliminated from the Hamiltonian for all open-ended ZDLs which define the character of the low-temperature transport. And this cancels the Hall current as well. Indeed, the above gauge transform shows that the effect of magnetic field on such a system will be null unless the ZGL are closed or are not single-connected. But in general the ZGL do not branch out. In fact, the presence of a branching point (x_0, y_0) means a simultaneous fulfillment of three conditions: $\Delta(x_0, y_0) = 0$, $\partial_{x_0}(x_0, y_0) = 0$ and $\partial_{y_0}(x_0, y_0) = 0$, which is practically impossible. Hence, the theory predicts a zero Hall current in the presence of magnetic field, in agreement with the experimental.

It worth noting that the bulk contribution to the Hall current will also be absent. Indeed, under these conditions the Fermi energy will be located in a narrow band of localized states. One can estimate this band width δ_b from the density interval $\delta n_s = 5 \times 10^9 \text{cm}^{-2}$ corresponding to the quenching of the Hall effect (see above). Using the value of DoS obtained from capacitance measurements [37] yields $\delta_b = 3 \text{meV}$. This estimate means that the band width of localized states is close to the characteristic disorder amplitude in HgTe quantum well.

METHODS

Quantum wells $\text{Cd}_{0.65}\text{Hg}_{0.35}\text{Te}/\text{HgTe}/\text{Cd}_{0.65}\text{Hg}_{0.35}\text{Te}$ with (013) surface orientations and a nominal well thickness of (6.3-6.6) nm were prepared by molecular beam epitaxy. As shown in the previous publications [9], the use of substrates inclined to the singular orientations facilitates the growth of more perfect films. Therefore, the growth of alloys is performed predominantly on the substrates with surface orientation [013], which deviates from the singular orientation by approximately 19° . Fabrication of ohmic contact to HgTe quantum well is similar to that for other 2D systems, such as GaAs quantum wells, for example: the contacts were formed by the burning-in of indium directly on the surface of large contact pads. Modulation-doped HgTe/CdHgTe quantum wells are typically grown at 180°C , which is relatively low compared to III-V compounds. On each contact pad the indium diffuses vertically down, providing ohmic contact to the underlying quantum well, with the contact resistance in the range of 0.1-1 kOhm. During the AC measurements we made sure

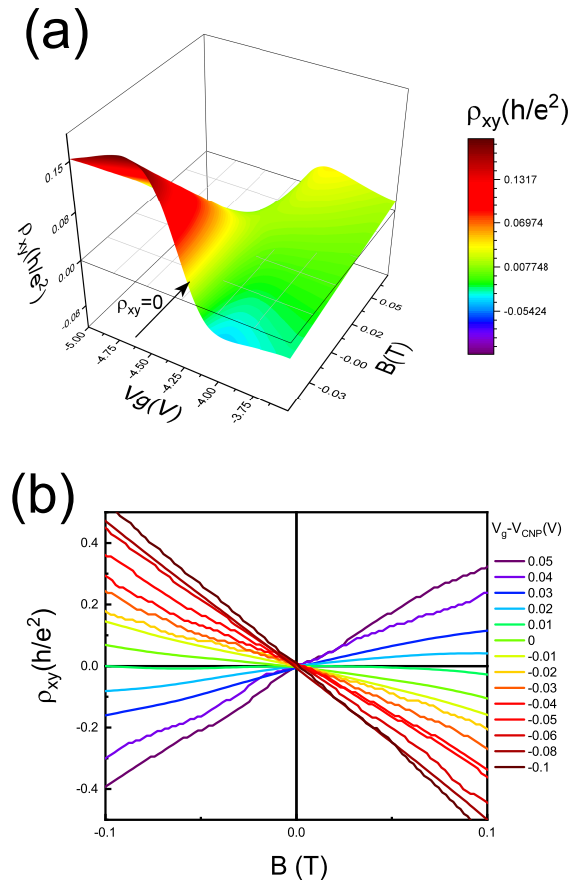


FIG. 5: (Color online) (a) The Hall resistivity as a function of the gate voltage and magnetic field near the CNP. (b) The Hall resistivity near the CNP for different values of gate voltage.

that the Y-component of the impedance did not exceed 5% of the total impedance, which is the indication of good ohmicity of the contacts. The sample is a Hall bar device with eight voltage probes. The bar has the width W of $50 \mu\text{m}$ and three consecutive segments of different lengths L (100, 250, 100 μm) (Figure 3, left bottom panel). A dielectric layer was deposited (100 nm of SiO_2 and 100 nm of Si_3Ni_4) on the sample surface and then covered by a TiAu gate. The density variation with gate voltage was $1 \times 10^{11} \text{cm}^{-2} \text{V}^{-1}$. The magnetotransport measurements were performed in the temperature 4.2K using a standard four point circuit with a 1 – 13 Hz ac current of 1 – 10 nA through the sample, which is sufficiently low to avoid overheating effects.

SUMMARY AND CONCLUSION

In conclusion, our results provide an opportunity to take a fresh look at the nature of electron transport in HgTe quantum wells of critical thickness. The descrip-

tion of transport in this system in terms of percolation through a network of one-dimensional conducting channels makes it possible to study the effects caused by the interplay of topology and localization. More generally, the study of transport in zero gap HgTe quantum wells can improve our understanding of the disorder induced topological insulator-to-metal transition and may be important for a wider class of disordered 2D electron systems, than was considered previously.

ACKNOWLEDGMENT

G.M. Gusev acknowledges for financial support FAPESP (Brazil) and CNPq (Brazil); Z. D. Kvon, D. A. Kozlov, E.B.Olshanetsky, M.V. Entin and N. N. Mikhailov acknowledge for financial support Ministry of Science and Higher Education of the Russian Federation, Grant No. 075-15-2020- 797(13.1902.21.0024).

References

-
- [1] Kane, C. L.; Mele, E. J. Z. Topological Order and the Quantum Spin Hall Effect. *Phys.Rev.Lett.* **2005**, *95*, 146802.
- [2] Hasan, M.Z.; Kane, C.L. Topological insulator. *Rev.Mod.Phys.* **2010**, *82*, 2045. Qi X-L., Zhang, S-C. Topological insulators and superconductors. *Rev.Mod.Phys.* **2011**, *83*, 1057.
- [3] Qi, X-L.; Zhang, S-C. The quantum spin Hall effect and topological insulators. *Phys. Today.* **2010**, *63(1)*, 33 .
- [4] Moore, J. E.; Balents, L. Topological invariants of time-reversal-invariant band structures. *Phys.Rev.B.* **2007**,*75*, 121306.
- [5] Moore, J.E. The birth of topological insulators. *Nature.***2010**, *464*, 194.
- [6] König, M.; Wiedmann, S.; Brune, C.; Roth, A.; Buhmann, H.; Molenkamp, L.W.; Qi, X.-L.; Zhang, S.-C. Quantum Spin Hall Insulator State in HgTe Quantum. *Science.* **2007**, *318*, 766.
- [7] Buhmann, H. The quantum spin Hall effect. *Journal. Appl.Phys.* **2011**, *109*, 102409.
- [8] Roth, A.; Brüne, C.; Buhmann, H.; Molenkamp, L.W.; Maciejko, J.; Qi, X.-L.; Zhang, S.-C. Nonlocal Transport in the Quantum Spin Hall State. *Science.***2009**, *325*, 294.
- [9] Gusev, G. M.; Kvon, Z. D.; Shegai, O. A.; Mikhailov, N. N.; Dvoretzky, S. A.; Portal, J. C. Transport in disordered two-dimensional topological insulators. *Phys. Rev. B.* **2011**, *84*, 121302(R).
- [10] Olshanetsky, E. B.; Kvon, Z. D.; Gusev, G.M.; Levin, A.D.; Raichev, O.E.; Mikhailov, N. N.; Dvoretzky, S. A. Persistence of a Two-Dimensional Topological Insulator State in Wide HgTe Quantum Wells. *Phys.Rev.Lett.* **2015**, *114*, 126802.
- [11] Rahim, A.; Levin, A. D.; Gusev, G. M.; Kvon, Z. D.; Olshanetsky, E. B.; Mikhailov, N. N.; Dvoretzky, S. A. Scaling of local and nonlocal resistances in a 2D topological insulator based on HgTe quantum well. *2D Materials.* **2015**, *2*, 044015.
- [12] Knez, I.; Du, R.-R.; Sullivan, G. Evidence for Helical Edge Modes in Inverted InAs / GaSb Quantum Wells. *Phys. Rev. Lett.* **2011**, *107*, 136603.
- [13] Knez, I.; Rettner, C. T.; Yang, S.-H.; Parkin, S. S. P.; Du, L.; Du, R.-R.; Sullivan, G. Observation of Edge Transport in the Disordered Regime of Topologically Insulating InAs/GaSb Quantum Wells. *Phys. Rev. Lett.* **2014**, *112*, 026602.
- [14] Du, L.; Knez, I.; Sullivan, G.; Du, R.-R. Robust Helical Edge Transport in Gated InAs/GaSb Bilayers. *Phys. Rev. Lett.***2015**, *114*, 096802.
- [15] Nichele, F.; Pal, A. N.; Pietsch, P.; Ihn, T.; Ensslin, K.; Charpentier, C. and Wegscheider W. Insulating State and Giant Nonlocal Response in an InAs/GaSb Quantum Well in the Quantum Hall Regime. *Phys. Rev. Lett.* **2014**, *112*, 036802.
- [16] Suzuki, K.; Harada, Y.; Onomitsu, K. and Muraki K. Gate-controlled semimetal-topological insulator transition in an InAs/GaSb heterostructure. *Phys. Rev. B.* **2015**, *91*, 245309.
- [17] Bernevig B. A. Topological Insulators and Topological Superconductors. Princeton University Press, 2013.
- [18] Masaru Onoda; Yshai Avishai and Naoto Nagaosa. Localization in a Quantum Spin Hall System. *Phys. Rev. Lett.* **2007**, *98*, 076802.
- [19] Hideaki Obuse; Akira Furusaki; Shinsei Ryu and Christopher Mudry. Two-dimensional spin-filtered chiral network model for the Z2 quantum spin-Hall effect. *Phys. Rev. B.***2007**, *76*, 075301.
- [20] Hideaki Obuse; Akira Furusaki; Shinsei Ryu and Christopher Mudry. Boundary criticality at the Anderson transition between a metal and a quantum spin Hall insulator in two dimensions. *Phys. Rev. B.***2008**, *78*, 115301.
- [21] Bondesan, R.; Gruzberg, I. A.; Jacobsen, J. L.; Obuse, H. and Saleur H. Exact Exponents for the Spin Quantum Hall Transition in the Presence of Multiple Edge Channels. *Phys. Rev. Lett.* **2012**, *108*, 126801.
- [22] Ai Yamakage; Kentaro Nomura; Ken-Ichiro Imura and Yoshio Kuramoto. Criticality of the metal-topological insulator transition driven by disorder. *Phys. Rev. B* **2013**, *87*, 205141.
- [23] Bhardwaj, S.; Mkhitarian, V. V.; Gruzberg, I. A. Supersymmetry approach to delocalization transitions in a network model of the weak-field quantum Hall effect and related models. *Phys. Rev. B.***2014**, *89*, 235305.
- [24] Chalker, J. T. and Coddington, P. D. Percolation, quantum tunnelling and the integer Hall effect. *J. Phys. C: Solid State Phys.***1988**, *21*, 2665.
- [25] Jian Li; Rui-Lin Chu; Jain, J. K. and Shun-Qing Shen. Topological Anderson Insulator. *Phys. Rev. Lett.* **2009**, *102*, 136806.
- [26] Mahmoodian, M. M. and Entin, M. V. Microwave Absorption in 2D Topological Insulators with a Developed Edge States Network. *Physica Status Solidi b.***2019**,*256*, 1800652.
- [27] Mahmoodian, M. M. and Entin, M. V. Conductivity of a two-dimensional HgTe layer near the critical width: The role of developed edge states network and random mixture of p-and n-domains. *Phys.Rev. B.***2020**, *101*, 125415.

- [28] Buttner, B.; Liu, C. X.; Tkachov, G.; Novik, E. G.; Brune, C.; Buhmann, H.; Hankiewicz, E. M.; Recher, P.; Trauzettel, B.; Zhang, S. C. and Molenkamp, L. W. Single valley Dirac fermions in zero-gap HgTe quantum wells. *Nat. Phys.* **2011**, *7*, 418.
- [29] Yahniuk, I.; Krishtopenko, S. S.; Grabecki, G.; Jouault, B.; Consejo, C.; Desrat, W.; Majewicz M.; Kadykov A. M.; Spirin K. E.; Gavrilenko, V. I.; Mikhailov, N. N.; Dvoretzky, S. A.; But, D. B.; Teppe, F.; Wróbel, J.; Cywiński, G.; Kret, S.; Dietl, T.; Wojciech Knap, W. Magneto-transport in inverted HgTe quantum wells. *npj Quantum Materials* **2019**, *4*, 13.
- [30] Kozlov, D. A.; Kvon, Z. D.; Mikhailov, N. N. and Dvoretzskii, S. A. Weak localization of Dirac fermions in HgTe quantum wells. *JETP Lett.* **2012**, *96*, 730.
- [31] Kozlov, D. A.; Kvon, Z. D.; Mikhailov, N. N. and Dvoretzskii, S. A. Quantum Hall effect in a system of gapless Dirac fermions in HgTe quantum wells. *JETP Lett.* **2014**, *100*, 724.
- [32] Gusev, G. M.; Kozlov, D. A.; Levin, A. D.; Kvon, Z. D.; Mikhailov, N. N. and Dvoretzky, S. A. Robust helical edge transport at $\nu = 0$ quantum Hall state. *Phys. Rev. B.* **2017**, *96*, 045304.
- [33] J. Davies, *The Physics of Low Dimensional Semiconductors*, Cambridge, 1997.
- [34] Dobretsova, A. A.; Kvon, Z. D.; Braginskii, L. S.; Entin, M. V. and Mikhailov, N. N. Mobility of Dirac electrons in HgTe quantum wells. *JETP Lett.* **2016**, *104*, 388.
- [35] Shklovskii, B. I.; Efros, A. L. *Electronic Properties of Doped Semiconductors*. Springer, Heidelberg, 1984.
- [36] Das Sarma, S.; Lilly, M. P.; Hwang, E. H.; Pfeiffer, L. N.; West, K.W. and Reno, J.L. Two-Dimensional Metal-Insulator Transition as a Percolation Transition in a High-Mobility Electron System. *Phys. Rev. Lett.* **2005**, *94*, 136401.
- [37] Kozlov, D. A. ; Savchenko, M. L; Ziegler, J.; Kvon, Z. D.; Mikhailov, N. N.; Dvoretzskii, S. A. and Weiss, D. Capacitance spectroscopy of a system of gapless Dirac fermions in a HgTe quantum well. *JETP Lett.* **2016**, *104*, 859.